A laboratory demonstration of solitons using a vertical watery conduit in syrup

John A. Whitehead
Department of Physical Oceanography, Woods Hole Oceanographic Institution, Woods Hole, MA 02543

(Received 26 March 1986; accepted for publication 30 December 1986)

Buoyant conduits of a water–syrup mixture were produced in syrup by injection from below. Low-amplitude waves on the walls of these conduits have been theoretically shown to obey the Korteweg–de Vries (KdV) equation which has soliton solutions. However, qualitative soliton behavior persists even for very-large-amplitude waves. Collision properties of two waves are compared to KdV solitons using video images of 16 collisions. Wave amplitude is conserved upon collison to better than $\pm 10\%$, but there is a slight enlargement of the large wave at the expense of the small wave. Position change in the trajectory of the waves due to wave–wave collision has the correct qualitative behavior when plotted against KdV theory. Wave packets that disperse into isolated solitary waves are also easy to observe.

I. INTRODUCTION

Solitary waves have been studied ever since John Scott Russell[1] followed on horseback a large solitary elevation along a channel in 1834. He named that "singular and beautiful phenomenon" the Wave of Translation and also coined the term "solitary wave," which is the term principally used by later investigators. He remained convinced of the singular nature of his great wave and carried out numerous experiments to observe the wave and its properties. He found, for instance, that a corresponding wave of depression does not exist.

A theoretical description of the wave emerged two decades later, when Boussinesq,[2] and soon thereafter Rayleigh,[3] found an isolated wave solution to the shallow water-wave equation. A decade later, Korteweg and de Vries[4] wrote down the governing equation for the surface elevation of the solitary wave that still bears their name:

$$\alpha_t + 6\alpha\alpha_x + \alpha_{xxx} = 0 \tag{1}$$

where the subscripts stand for differentiation with respect to that variable. It possesses the solution

$$\alpha(x,t) = 2C^2 \operatorname{sech}^2[C(x - 4C^2 t)]. \tag{2}$$

Three decades later it was found that the solutions retain their shape even after interaction with other disturbances. Isolated waves with this property have come to be called "solitons." Theoretically, solitons are associated with a large class of eigenvalue problems that possess evolution equations with invariant spectra. Solitons retain their shape upon collision, but their trajectory in space-time experiences a displacement (often called a phase change). Although there are wide classes of soliton equations, the Korteweg–de Vries equation, commonly abbreviated as the KdV equation, is one of the simplest and most common soliton equations.

Solitons occur in many physical systems but experiments to observe them have been either elaborate, as in plasma physics, or large, as in hydraulics. For instance, excellent observations in water waves were made by Hammack and Segur,[5] who used a wave tank 31.6 m long, 61 cm deep, and 39.4 cm wide. Data were recorded with parallel wire resistance gauges and an oscillograph recorder.

We report here a simple tabletop experiment that has solitary waves with properties close to those of a soliton. It is suitable for a physics laboratory project or a classroom demonstration. Collision properties and the behavior of packets can be recorded and analyzed with photography, video tape, or demonstrated in real time. The flow and scaling laws are also readily written down. The equations reduce to the KdV equations in the limit of small amplitude,[6] but experimentally, the waves most easily observed have larger amplitude. Interestingly, they still approximate solitons.

The experiment is very simple. It follows an earlier experiment by Whitehead and Luther[7] and involves a water and corn syrup mixture being injected at the bottom of a tank filled with corn syrup. The injected mixture first accumulates around the source as a growing sphere. After a brief time the sphere is large enough to rise away buoyantly from the source at a speed faster than the rate of change of the radius. At that time, it appears to detach from the source and float upward. The injected fluid now rises to the ascending sphere through a cylindrical conduit (sometimes called a pipe), which is typically much smaller than the sphere. Subsequently, the sphere rises to the top and the conduit stretches from bottom to top. The radius of the conduit can be calculated using a simple balance between buoyancy and viscous forces. It depends on the following parameters: Q—the volumetric flow rate, ν—viscosity of the injected fluid, g—acceleration due to gravity, and $\Delta\rho/\rho$—the normalized density difference between the ambient and injected fluid. For the remainder of this article we will define $g' = g\Delta\rho/\rho$.

The formula for the radius of the conduit is

$$r_c = (4\nu Q/\pi g')^{1/4}. \tag{3}$$

When the volume flux into the conduit is temporarily increased, solitary waves are formed. The wave equations are[8]

$$\frac{\partial A}{\partial t} = -\frac{\partial Q}{\partial z}, \tag{4}$$

$$Q = \frac{A^2}{8\pi\nu}\left(g' + \nu_o \frac{\partial}{\partial z}\frac{1}{A}\frac{\partial Q}{\partial z}\right), \tag{5}$$

where $A = \pi r^2$ is the cross-sectional area of the conduit. The subscript o denotes properties of the ambient (or outer) fluid, c denotes geometric properties of the conduit, and no subscript denotes the properties of the injected fluid.

 © 1987 American Association of Physics Teachers

Equations (4) and (5) reduce in the small (but finite) amplitude limit to the KdV equation,[6] which in dimensional form is

$$\frac{\partial A'}{\partial t}+\frac{g'A_c}{4\pi\nu}A'\frac{\partial A'}{\partial z'}+\frac{g'\nu_o A_c^2}{32\pi^2\nu^2}\frac{\partial^3 A'}{\partial z'^3}=0. \quad (6)$$

Here the coordinate z' is moving with the linear wave speed

$$C_l=g'A_c/4\pi\nu \quad (7)$$

and A' is deviation from A as defined in Eq. (8). The solution to Eq. (6) is

$$A'=\frac{A-A_c}{A_c}=\frac{A_m-A_c}{A_c}\times\operatorname{sech}^2\left[\frac{2}{r_c}\left(\frac{(A_m-A_c)\nu}{A_c\nu_o}\right)^{1/2}(z'-C_p t)\right] \quad (8)$$

with propagation speed

$$C_p=g'(A_m-A_c)/12\pi\nu, \quad (9)$$

where A_m is the cross-sectional area of the solitary wave at its widest part. Solitary wave solutions to the full Eqs. (4) and (5) are also known[9] and are

$$A=A_m\exp\left(\frac{[-(8\pi\nu/A_o\nu_o)^{1/2}z-2\ln(A_m/A_o)g'(A_o/8\pi\nu\nu_o)^{1/2}t]^2}{2\ln(A_m/A_o)}\right), \quad (10)$$

but they have not been shown to be solitons. Laboratory observations of large solitary waves in these conduits have seemed to be conserved when they collide,[8] like solitons. The experiment described in Sec. III reports measurements of collision properties close to those of solitons even though their amplitude is beyond the range that could justify the derivation of the KdV equation according to Whitehead and Helfrich.[6]

II. PREPARATION

The apparatus is very similar to that with which conduits were first observed by Whitehead and Luther in 1974. Figure 1 shows a sketch. Karo syrup (a commercial corn syrup widely available in the U.S.) was put into a Plexiglass container 11 cm thick by 20 cm wide by 69 cm deep. The syrup has a density $\rho_o=1.34$ g/cm^3, and a viscosity $\nu_o=41.0$ cm^2/s. After pouring, it was necessary to leave the syrup overnight to allow air bubbles to rise out. Other syrups or oils could be used as well; the author has used silicon oil, golden syrup (in Britain), and a commercial corn syrup bought in bulk. Scott *et al.*[8] used honey with

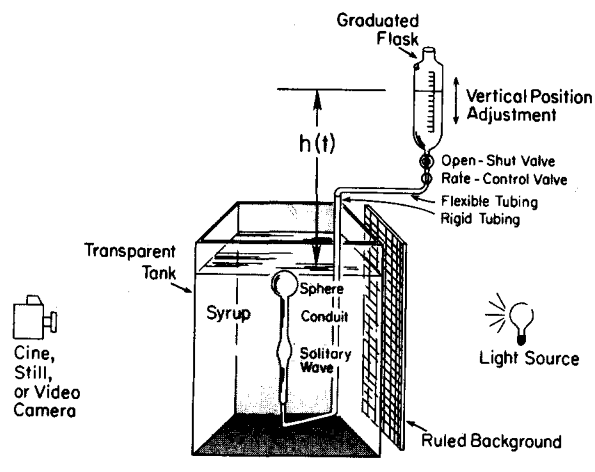

Fig. 1. Sketch of the experimental apparatus and the visualization system. The head $h(t)$ is adjustable so the flow rate of the injected fluid can be varied.

equal success. Glycerine is to be avoided as it has peculiar hygroscopic properties that result in nonlinear water–glycerine diffusivities and a suspect wall condition for the conduit.

The injected fluid was a 70–30 mixture (by volume) of syrup and water, with density $\rho=1.24$ g/cm^3 and viscosity $\nu=0.5$ cm^2/s. As a practical note, it is best to add the syrup to the water for mixing; otherwise, it is difficult to mix completely the viscous fluid next to the wall. To observe the conduit, the injected mixture was dyed with food coloring. The mixture was injected through a hollow tube approximately 1.5 mm i.d. We found hypodermic syringe tubing to be convenient, and Olson and Christensen[9] used glass. The tubing was connected by hose to a 50-cm^3 graduated reservoir mounted beside the tank. In practice, it was important to keep the injector outside the test container until the run was to start. Otherwise, clogging by the viscous corn syrup made starting very difficult. The reservoir was placed beside a meter stick whose zero was at the level of the ambient fluid. With this, the surface of the injected fluid could easily be set anywhere from 0 to 100 cm above the level of the tank. Scott used a motorized syringe injector and it had no clogging problems.

Records of the waves were made with both taped video camera and 35-mm pictures. The diameter of the conduit was then easily measured as a function of vertical position and time; thus the amplitude, shape, and position of the solitary waves could be determined. The only necessary additional preparations were the marking and mounting of a background with a centimeter scale and proper lighting. We selected back lighting aimed directly onto translucent graph paper from behind the tank. This yielded precise images of the outline of the conduit on a calibrated background.

To start the runs, the injector tube was lowered into the tank and clamped into place. The reservoir surface was then quickly raised 100 cm above the ambient fluid surface so that a great flux of injected fluid entered at the bottom of the tank. The initial sphere grew to a large size and rose straight up to the top of the tank. In this way the conduit that followed the sphere was initially nearly vertical. The reservoir surface was then placed 6 cm above the ambient fluid surface, and a steady laminar conduit of approximately 2.0 mm diameter could be maintained as long as the reservoir was faithfully replenished. The conduit would sometimes slowly bend, probably due to convection in the tank from the floodlights. The bend may be responsible for a troublesome variation in the wave speed along the conduit in some runs, and we advise caution in using floodlights near the tank.

After some trial and error, we found that reproducible solitary waves could be generated by lifting the reservoir from the 6-cm height to a greater (varying from 5 to 90 cm) height for 4 s and then returning it to 6 cm. With a bit more practice, two waves could be made, with the smaller one first and the larger one second, so they collided near the middle of the tank. The video camera, which had a zoom lens, was operated by a cameraman, so that the field of view could be confined to the area of immediate interest. In this way we found that the video system data were comparable in accuracy to those of the 35-mm camera, which photographed the whole tank.

III. MEASUREMENTS

We will describe a typical project that has been done with solitary waves on these conduits. An attempt was made to measure the position jump, or so-called phase change, that the trajectory of solitons experiences upon collision. In order to obtain a measure of the relation between amplitude and position jump, 16 runs were conducted. They yielded useful data over the range of wave amplitudes shown in Table I.

The collisions appear at first sight to faithfully mimic the Korteweg–de Vries soliton behavior. Figure 2 shows photographs of two collisions. The first involves waves of very different amplitude and the second involves waves with similar amplitude. In both cases the faster (larger) wave overtakes the slower (smaller) wave and pumps fluid into it when they touch. After the two symmetrically exchange their volume difference, the first wave, which is now the larger, propagates ahead and away from the trailing wave, which is now smaller. The overall result of the collision is a position jump in the trajectory of each solitary wave. Scott, Stevenson, and Whitehead[8] give a similar description of the collision of these solitary waves and Scott and Stevenson[10] observed the same behavior in their computations (see their Fig. 3). The same features are shown in many textbooks, for instance in Lamb[11] and Newell.[12]

Table I. Results of the experiments on collisions of two solitary waves. The symbol a_{ij} is diameter of the wave, θ_i is the measured position jump, and C/d_i is the position jump predicted by Eq. (11). Subscript $i = 1,2$ denotes large or small wave, and $j = 1,2$ denotes before or after the collision. Runs 1, 2, 8, 9, and 14 on 23 Jan. resulted in no collision.

Run	Date	a_{11} (cm)	a_{12} (cm)	θ_1 (cm)	C/d_1 (cm)	a_{21} (cm)	a_{22} (cm)	θ_2 (cm)	C/d_2 (cm)
3	(23 Jan. 86)	0.53	0.53	1.7	0.26	0.35	0.36	1.7	0.70
4		0.65	0.65	1.7	0.31	0.54	0.49	2.5	0.48
5		0.71	0.66	2.3	0.20	0.47	0.51	2.5	0.41
6		0.61	0.64	2.5	0.35	0.52	0.50	2.5	0.55
7		0.63	0.62	2.0	0.19	0.46	0.41	2.1	0.50
10		0.55	0.56	???	0.37	0.48	0.41	???	0.70
11		0.58	0.70	2.0	0.30	0.55	0.47	1.6	0.50
12		0.58	0.75	1.8	0.11	0.42	0.36	2.0	0.41
13		0.64	0.68	1.8	0.09	0.39	0.32	2.5	0.41
15		0.60	0.70	0.8	0.01	0.24	0.20	2.1	0.42
16		0.68	0.66	1.4	0.03	0.30	0.24	1.7	0.39
1	(28 Jan. 86)	0.63	0.71	0.7	0.03	0.26	0.26	???	0.39
2		0.65	0.68	0.7	0.05	0.29	0.29	1.3	0.41
3		0.58	0.57	2.5	0.47	0.51	0.49	2.3	0.67
4		0.64	0.64	2.7	0.57	0.62	0.59	2.5	0.71
5		0.64	0.65	2.3	0.47	0.60	0.59	2.5	0.62

IV. ANALYSIS OF DATA

The sequence described in Sec. III was apparent in all our runs as shown in the trajectories of the waves in space-time (Fig. 3). To acquire these data, the video tape was played and the time when the waves were at each 5-cm division was recorded with a lap timer sports watch. The trajectories were similar to those expected for KdV collisions, but they differed in some important practical ways. Primarily, the velocity of the waves was not strictly constant. When we originally attempted to measure the position shifts, the position of the waves was plotted and a straight line was drawn through them. The extrapolated lines were expected to lag behind the leading wave and lead the trailing wave after the collision. However, no clear results were obtained with our data. Upon close inspection, a curvature of the trajectories was discovered due to a slight decrease in velocity of each wave with height in the 23 January runs. In the 28 January runs, pains were taken to make the conduit more nearly vertical by moving the floodlights further away from the tank and hence decreasing convection. The runs were also conducted as soon as possible after the initiation of the conduit to ensure that the conduit was as vertical as possible. In these runs the change in velocity of waves along the conduit was substantially less and the final observations had less scatter.

In order to determine changes in the relative positions of the waves after collision, it was vital to correct for the decrease in velocity with height that the 23 January runs exhibited. To do this, the trajectory of a wave close to the same amplitude from either run 8 or 9, which had no collision, was superimposed on the data. The trajectory was matched to the first four or five points of the precollision wave and the curve was drawn. For cases where run 8 or 9 did not provide the proper reference wave speed, the trajectory of one of the waves from run 9 was used with artificially stretched time. The results are shown in Fig. 3 and they clearly show measurements of the position change. All the measurements are shown along with amplitudes in Table I.

Three methods were tried to measure the width of the wave at the widest part of the conduit: First, divider measurements were taken from a stopped video tape image on a video monitor. The dividers where then measured with an optical micrometer precise to ± 0.1 mm. Second, optical micrometer measurements were taken directly from the monitor. Third, optical micrometer measurements were taken from a 35-mm slide projector. In theory, the slide had approximately 20 times better absolute resolution and should have been inherently superior, but in fact the video-caliper method had many advantages: First, the fact that the camera operator zoomed onto the area of interest was responsible for producing absolute resolution comparable to or better than the film. Second, we could alter the color hue, intensity, and contrast of the monitor to determine more precisely the location of the edge of the wave. Third, the calipers could be carefully adjusted with little eyestrain to allow extremely objective measurements whose quality

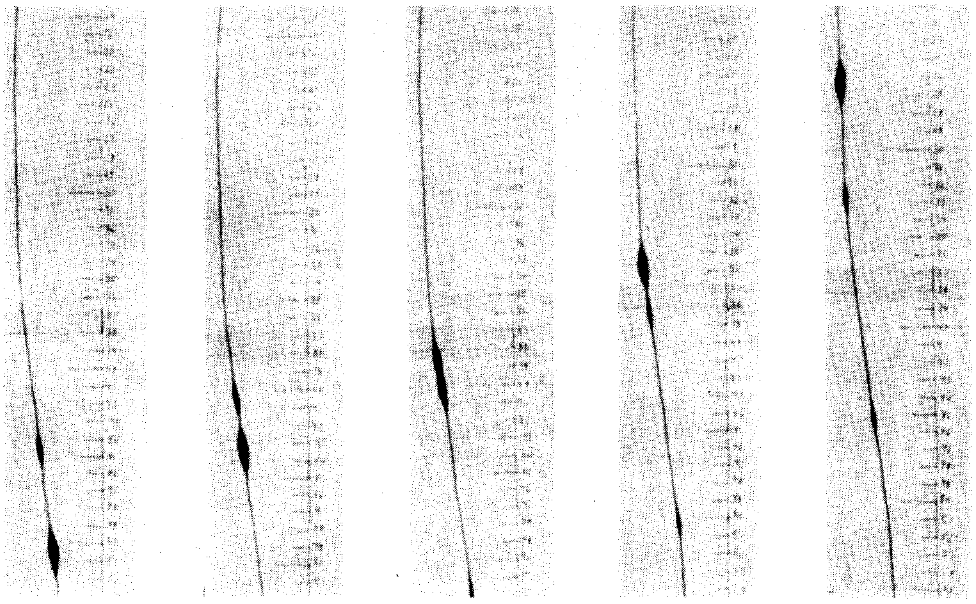

(a)

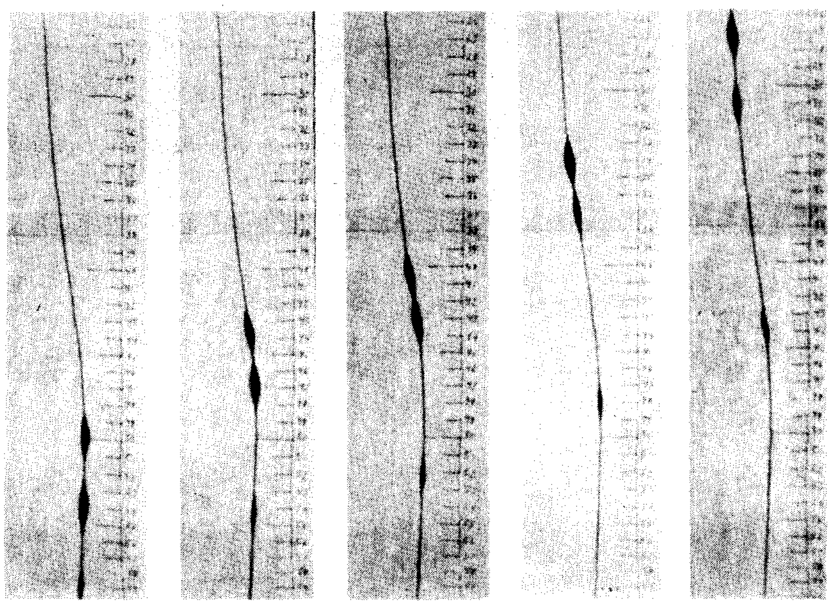

(b)

Fig. 2. Photographs of some of the solitary wave collisions. (a) A collision between a very large and a very small solitary wave. This is run 13 on 23 Jan. Times after first frames are 10, 15, 20, and 35 s, respectively. (b) A collision of two waves whose amplitude and speed are nearly the same. This is run 6 on 23 Jan. Times after the first frame are 10, 15, 25, and 35 s, respectively.

was uniform for all measurements. Fourth, it was not necessary to work in a darkened room.

Figures 4, 5, and 6 show the results. Figures 4 and 5 have position change plotted against a relation from the Korteweg–de Vries formula[13]

$$\frac{C}{d_i} = -2 \ln\left(\frac{d_1 - d_2}{d_1 + d_2}\right) / d_i, \tag{11}$$

where d_i is diameter of the ith wave. There is no known mathematical relation between this formula and Eq. (6), since here we use diameter and in (6) the area of the conduit is the variable. Fits of the data against a variety of empirical formulas were tried and this simply gave the best fit.

The least-squares fits correlation coefficients are given in the captions. In both cases there was considerable scatter. There is systematic dependence upon C/d_i of the position change of trajectory of the larger wave, but there is almost no dependence of the position change of the trajectory of the smaller wave with C/d_i.

The amplitude of the waves before and after collision is shown in Fig. 6. The conservation of amplitude after collision is not verified in detail and it appears that in general the large waves get a little larger and the small waves get a little smaller. Virtually all data exhibited enlargement of the large wave at the expense of the small one as indicated by the slope of 0.717 in the least-squares fit. The correlation coefficient of 0.92 is statistically significant at the 95% confidence level. The slope of the least-squares fit for the 28 January data is 0.92 and the correlation coefficient is 0.98, which is statistically significant at the 99% confidence level.

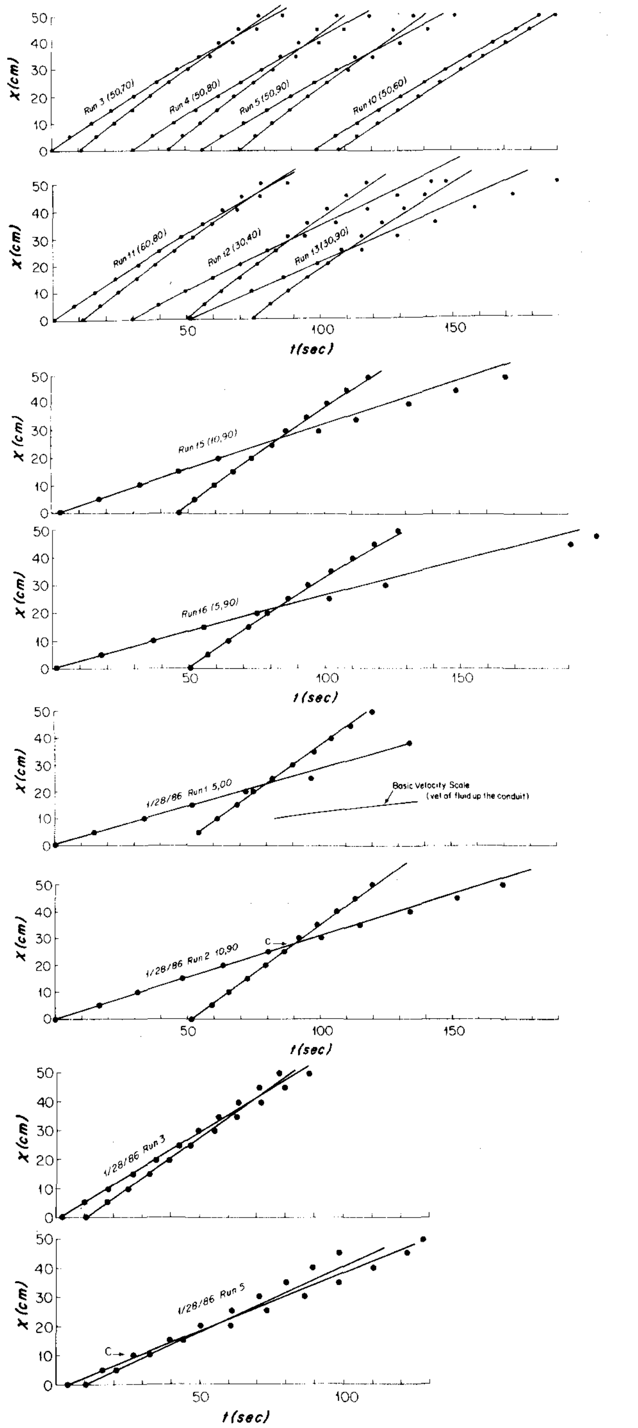

Fig. 3. Experimental values of the trajectories of the waves in 13 of the runs. For purposes of measuring the position change of the trajectory after collision, curves have been drawn which show the trajectory of a wave of similar amplitude in the absence of a collision.

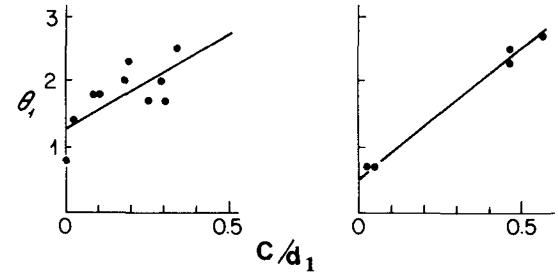

Fig. 4. Position change of the larger waves as a function of the parameter in C/d from Eq. (11). The line of least-squares fit is given. The 23 Jan. data are on the left. The least-squares fit is $\theta_1 = 2.77\, C/d_1 + 1.28$ and the correlation coefficient is $r = 0.71$. The 28 Jan. data are on the right. The least-squares fit is $\theta_1 = 3.86\, C/d_1 + 0.55$ and the correlation coefficient of the fit is 0.996. The first is statistically significant at the 95% confidence level and the second at the 99% confidence level.

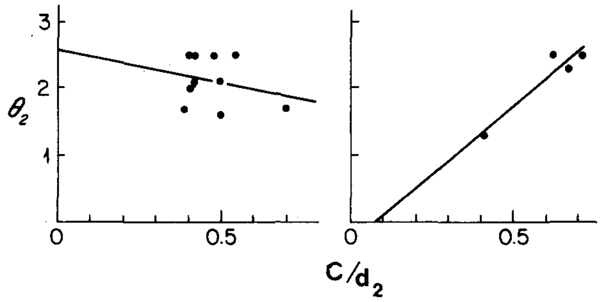

Fig. 5. Position change of the smaller waves as a function of the parameter C/d_i from Eq. (11). The line of least-squares fit is given. The 23 Jan. data are on the left. The least-squares fit is $\theta_2 = -1.20\, C/d_2 + 2.61$ and the correlation coefficient is $r = -0.26$. The 28 Jan. data are on the right. The least-squares fit is $\theta_2 = 4.06\, C/d_2 - 0.30$ and the correlation coefficient is 0.95. The left-hand data do not statistically satisfy a linear fit at the 95% confidence level but the right-hand data do.

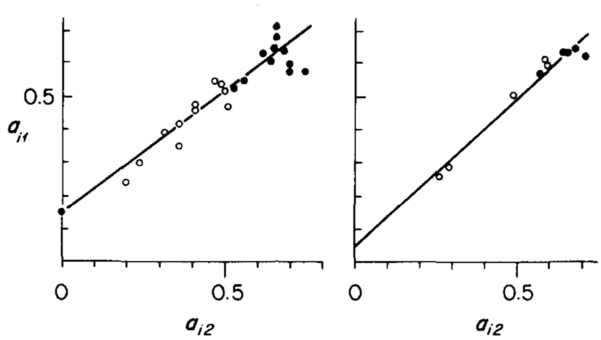

Fig. 6. Amplitude of the waves before (ordinate) and after (abscissa) the collisions. The open circles denote the small waves and the closed circles denote the larger waves. The 23 Jan. data are on the left. The least-squares fit is $a_{i1} = 0.717 a_{i2} + 0.15$ and the correlation coefficient is 0.92. The 28 Jan. data are on the right and the least-squares fit is $a_{i1} = 0.92 a_{i2} + 0.04$. The correlation coefficient is 0.981. Both are statistically significant at the 99% confidence level. This is clear evidence that large waves become larger and small waves become smaller after collision. Thus the waves do not unambiguously behave like solitons.

Other projects involving these waves are possible. One of the more interesting experiments is to observe the dispersion of a packet of solitary waves. Figure 7 shows a packet of waves in a conduit of very small size. The waves were initially connected, but break into five totally separate solitary waves. More advanced students could compare such packets with inverse scattering theory, as done for instance by Hammack and Segur[5] (see also Whitham[14] for help in the calculations).

V. SUMMARY AND CONCLUSIONS

Solitary waves were conveniently made in a simply constructed apparatus and were recorded on video tape. Amplitude was conserved after the collision to better than $\pm$ 10% for most of the data. There is a slight enlargement of the large wave at the expense of the small wave. The collisions produced clear position changes in the trajectories that roughly correlated with a realization of the expected KdV form. Solitonlike packets can also be produced and measured.

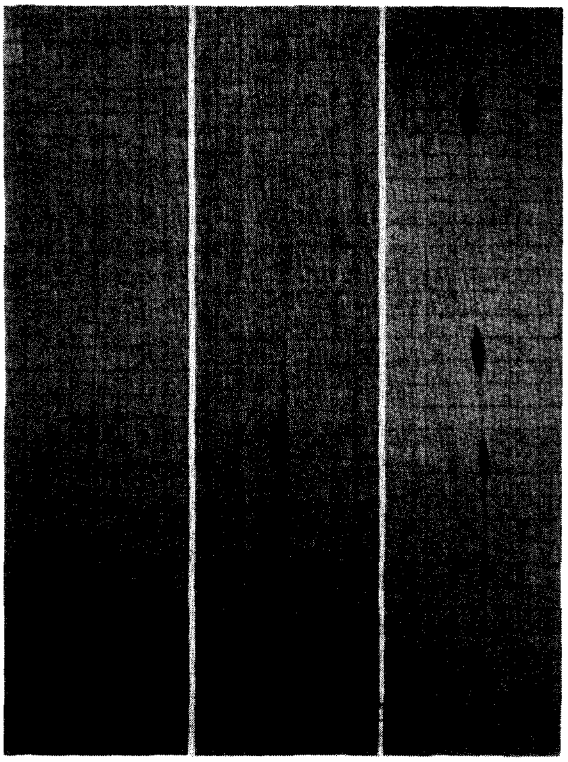

Fig. 7. Photographs of a packet of five waves from an initial closely connected state. They evolved to their ultimate state of five unconnected solitary waves.

VI. APPLICATIONS

Conduits like those described here have recently become of interest in geology and geophysics. They possibly exist in the mantle of the Earth to allow heat to escape upward through the viscous mantle of the Earth as "hotspots." They may also be considered analogs of melt rising buoyantly through a matrix of crystals where the mantle of the Earth partially melts[7,9,10]; the conduit fluid of our apparatus is equivalent to the melt, the ambient syrup is equivalent to the viscous crystalline matrix, and the cross-sectional area of the conduit is equivalent to the porosity of the crystal matrix. Conduits may also be important in magma chambers where new magma is injected into denser and more viscous magma.[15]

ACKNOWLEDGMENTS

Support for the study of geological applications of conduits comes from the Center for the Analysis of Marine Systems of Woods Hole Oceanographic Institution. The author investigates isolated eddies in ocean models under Grant OCE-8416100 from the National Science Foundation. The experience and equipment for this experiment arose from that support. Thanks are due to Wendy Smith for serving as cameraman, to Karl Helfrich for discussions concerning the theory and scaling, and Robert Frazel for the photography. Woods Hole Oceanographic Contributions number 6185.

[1] J. S. Russell, *Fourteenth Meeting of the British Association for the Advancement of Science*, (Murray, London, 1844), pp. 311–390 + 57 plates.
[2] J. Boussinesq, J. Math. Pures Appl. **17**, 55 (1872).
[3] Lord Rayleigh, Philos. Mag. **5**, 257 (1876).
[4] D. J. Korteweg and G. de Vries, Philos. Mag. **39**, 422 (1895).
[5] J. L. Hammack and H. Segur, J. Fluid Mech. **65**, 289 (1974).
[6] J. A. Whitehead and K. Helfrich, Geophys. Res. Lett. **13**, 545 (1986).
[7] J. A. Whitehead and D. S. Luther, J. Geophys. Res. **80**, 705 (1975).
[8] D. R. Scott, D. J. Stephenson, and J. A. Whitehead, Nature **319**, 759 (1986).
[9] P. Olson and U. Christensen, J. Geophys. Res. **91**, 6367 (1986).
[10] D. R. Scott and D. J. Stephenson, Geophys. Res. Lett. **11**, 1161 (1984).
[11] G. L. Lamb, Jr., *Elements of Soliton Theory* (Wiley, New York, 1980), Fig. 4.4.
[12] A. C. Newell, *Solitons in Mathematics and Physics* (Society for Industrial and Applied Mathematics, Philadelphia, PA, 1985), p. 83.
[13] Reference 12, p. 83. Here we have replaced A with C and η with d to avoid confusing notation.
[14] G. B. Whitham, *Linear and Nonlinear Waves* (Wiley, New York, 1974), pp. 577–599.
[15] H. E. Huppert, R. Stephen, J. Sparks, J. A. Whitehead, and M. A. Hallworth, J. Geophys. Res. **91**, 6113 (1986).

Relativistic and nonrelativistic Kronig–Penney models

F. Domínguez-Adame

Departamento de Física de la Materia Condensada, Facultad de Ciencias Físicas (U.C.M.), 28040-Madrid, Spain

(Received 25 September 1986; accepted for publication 19 February 1987)

The wavefunction and the Kronig–Penney dispersion relation of an electron moving in a one-dimensional periodic array of delta potentials are found, in the relativistic as well as in the nonrelativistic case. The Green's function method and Bloch's theorem are used in a simple form.

I. INTRODUCTION

The Kronig–Penney model[1] has been widely used to introduce some important concepts of electron dynamics in a periodic potential, namely, Bloch functions and the occurrence of energy bands. This model assumes a single electron moving in one-dimensional periodic square well potentials. However, this potential is frequently replaced by a

© 1987 American Association of Physics Teachers